

# Corrosion Characterization of Friction Stir Weld Dissimilar Aluminium Alloy Joints

K Ramesha<sup>a</sup>, Santhosh N<sup>b</sup>, Naresh H<sup>c</sup>

<sup>a</sup>Department of Mechanical and Automobile Engineering, CHRIST (Deemed to be University), Bengaluru, Karnataka, India. E-mail: [ramesha.kra@gmail.com](mailto:ramesha.kra@gmail.com)

<sup>b</sup>Dept. of Mech. Engg., MVJ College of Engg., Bengaluru, Karnataka, India, E-mail Id: [santhoshnagaraja@gmail.com](mailto:santhoshnagaraja@gmail.com)

<sup>c</sup>Dept. of Mech. Engg., Siddaganga Institute of Technology, Tumakuru, Karnataka, India. Email Id: [nareshh@sit.ac.in](mailto:nareshh@sit.ac.in)

## Abstract

The course of contact mix welding is quick acquiring conspicuousness in aviation, marine and car industry because of its benefits as far as mechanical strength, effect and hardness characteristics. There is as yet a requirement for sure fire consideration from the exploration local area to erosion in grating mix welding zones, hence the work introduced here centres around the consumption portrayal of the grinding mix weld divergent aluminium composite. This study looks into friction stir welding under various parametric settings and shows how corrosion happens in a sodium chloride electrolytic media under potentio-dynamic conditions. The friction stir weld joints of dissimilar alloys aluminium are constructed using three sets of parameters. Straight cylinder, taper cylinder, and straight triangular tool profiles; tool rotational speeds of 800, 1000, and 1200 rpm; tool feed rates of 100, 120, and 140 mm/min; and tool offsets of 0.5, 0 mm, and -1.5 mm. The corrosion current ( $I_{corr}$ ) reduces as tool rotating speed increases up to 1200 rpm, after which it slightly increases due to the creation of ridges all around the periphery of the friction stir weld area.

**Keywords:** Potentiodynamic, Aluminium Alloys, Characterization, Corrosion, Friction Stir Welding, Dissimilar.

## 1.0 Introduction

Friction stir welding (FSW) is a solid-state welding technique that includes combining work pieces using a non-consumable tool that softens the metal by creating heat by friction between both the rotating tool and the work piece [1,2,3, and 4]. When the tool rotates inside the work piece, it deforms the material plastically, resulting in a strong joint. FSW welding of aluminium and related alloys is rapidly gaining popularity, particularly in aerospace and vehicle components. As a result, the current research focuses on the welding of different aluminium alloys [AA (Aluminium Association) 5xxx series and AA 7xxx series alloys].

The light metal alloys AA 7xxx and AA 5xxx are most typically utilised in numerous structural

applications, particularly in the aerospace, marine, and car sectors.

When these materials are utilised to build various structural components, the overall weight is reduced, which improves fuel economy and reduces pollution [5, 6]. Due to the development of high temperatures, the combining of different aluminium alloys using the traditional fusion welding process leads in the formation of intermetallic compounds and numerous welding related flaws [7-9].

Corrosion characterisation of weld joints has become more important as a result of the world's increasing need to conserve metal supplies [10]. Researchers have paid close attention to corrosion studies of friction stir weld dissimilar aluminium alloys because of their real-time applications in the aerospace and automotive industries [11, 12].

Aluminium and aluminium alloys had already established themselves as important materials in a wide range of applications [13]. The majority of research on corrosion of several metals and alloys in HCl and H<sub>2</sub>SO<sub>4</sub> media have been published, but none on corrosion in NaCl media [14, 15]. Hence this gap in available literature has given scope for evolving interest in potentiodynamic corrosion characterization of the friction stir weld specimens in sodium chloride (NaCl) media.

## 2.0 Materials and Methods

### 2.1 Work Piece Material

Friction stir welding is used to join different aluminium alloys, such as AA 7075 and AA 5052; the composition of the alloys used in this study is listed in Table 1. Availability of the required fixture specifications to hold the work piece, the work piece is cut to the size needed of 170\*60\*5 mm, as illustrated in Figure 1.

The aluminium alloy AA 7075, was chosen for this study because it has high strength, corrosion resistance and fracture toughness, which is a significant quality for its usage in aerospace structures, whereas the AA 5052 aluminium alloy with magnesium as a primary alloying element has

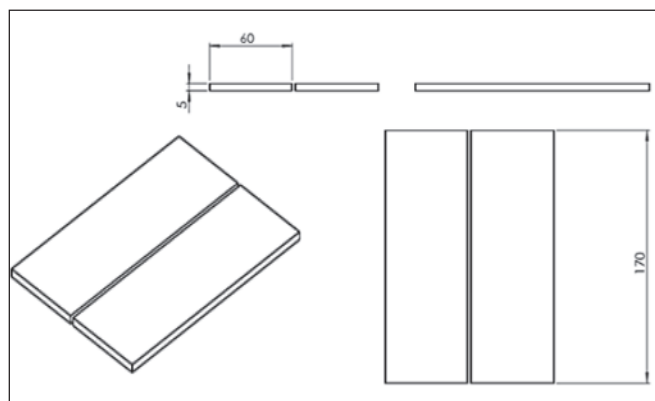


**Figure 1:** Schematic of the workpiece used in the present work

greater strength, weldability, and corrosion resistance, which is a key component in its adoption inside this research to optimise the processing parameters of the FSW for plate frameworks.

### 2.2 Tool Material

A non-consumable tool manufactured of H13 tool steel with a hardness of 55 HRC is used for friction stir welding. The tool's parameters are shown in Table 2. This research looked at three pin shapes: cylindrical, cylindrical taper, and triangular; a schematic of the three pin profiles is presented in Figure 2.

Table 2: Tools Specification	
Tool shoulder	20 mm (flat surface)
Tool pin configuration	Cylindrical, Cylindrical Taper, and Triangular
Pin length	4.8 mm
Pin Size	Cylindrical D = 05 mm
	Triangle L = 05 mm
	Taper D = 05 mm
	d = 04 mm

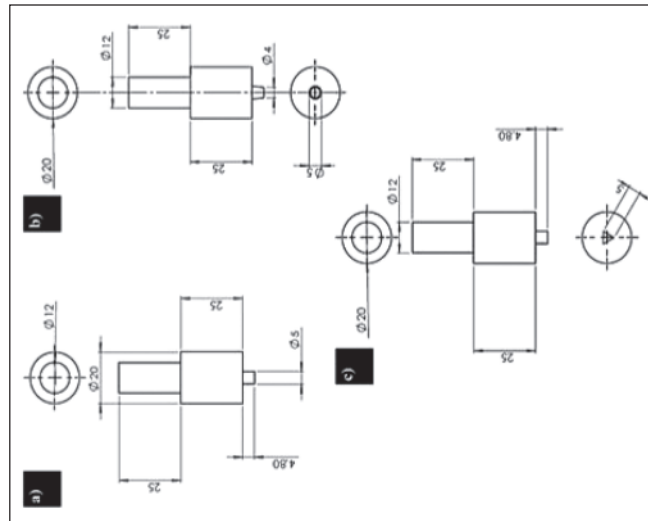


**Figure 2:** Schematic of the tools pin profiles (a) Cylindrical (Cyl.) (b) Cylindrical – taper (Cyl. Tp.) and (c) Triangle

Table 1: AA 7075 and AA 5052 alloys Composition

Elements (Wt.%)	Al	Zn	Mg	Cu	Si	Fe	Cr	Mn	Ti	Others
AA 7075	Bal.	5.80	2.40	1.60	0.40	0.40	0.250	0.20	0.10	0.140
AA 5052	Bal.	0.10	2.60	0.10	0.450	0.350	0.20	0.10	-	0.150

**Table 3: Levels of Parameters Considered for FSW**

	Parameters	Level I	Level II	Level III
1.	Tool Pin Profile	Cylindrical	Cylindrical (Taper)	Triangle
2.	Tool Offset (mm)	-0.50	00	0.5
3.	Rotational Speed (rpm)	0800	1000	1200
4.	Feed (mm/min)	0100	0120	0140

### 2.3 Experimental-Method

AA 7075 and AA 5052 alloys are friction stir welded together on an ETA manufacture 10 T type horizontal FSW equipment. The technique is carried out using Minitab Software's Design of Experiments (DOE) table, which is framed using the L9 orthogonal array and the Taguchi Design model considering 3 factors  $\times$  3 level interactions. This study looked at design-specific aspects such rotation speed (800, 1000, and 1200 rpm), transverse feed (80, 100, and 120 mm/min), and tool pin arrangement (cylinder, cylinder-taper, and triangle). Table 3 details the welding parameters and their levels. The welding procedure has Al 7075 on the receding side and Al 5052 on the advancing side. The tool shoulder is sunk into plates affixed to specific fixtures clamped to the machine's table, and the FSW procedure is performed according to the Design of Experiments (DOE) [15, 16].

Further, the friction stir weld specimens are subjected to corrosion in saline medium, especially to evaluate the corrosion characteristics of the weld joints in electro potential environments. The tests are carried out in accordance with the ASTM G 102, G 59 and G 5 standards to determine the corrosion current and the corrosion rate.

These test methods are utilized to experiment, verify and validate the polarization resistance and potential measurements involving the critical aspects of electrochemical potentials, measuring and recording processes. The test method involves experimental techniques for polarization resistance measurements and subsequent potential measurements.

### 2.4 Preparation of NaCl solution

A 3.5 M sodium chloride (NaCl) medium stock solution is generated using 204.54 g of analytical grade Sodium Chloride (NaCl salt) and double distilled water. The potentiometric approach is used to standardise it. In a 1 litre capacity beaker, place the desired amount of sodium chloride and add distilled water until the solution reaches the 1 litre graduated point. The solution is agitated once more, and the saline corrosion medium is created for use as an electrolytic medium.

### 2.5 Potentio-dynamic Corrosion Characterization

The Potentio-dynamic corrosion characterization calculates the corrosion current and rate for various friction stir weld specimens. Figures 3, 4, and 5 show

**Table 4: Corrosion values for FSW specimens**

Exp. No.	Rotational Speed (RPM)	Feed (mm/min)	Tool Offset (mm)	Tool Pin Profile	Icorr (E-4) A	Corr. Rate (E-2)g/mV
1	800	100	0	Cyl.	6.228	5.816
2	800	120	0.5	Cyl.(Tp)	6.332	5.924
3	800	140	-0.5	Tr.	6.689	6.212
4	1000	100	0	Cyl.	1.363	0.957
5	1000	120	0.5	Cyl. (Tp.)	2.424	1.998
6	1000	140	-0.5	Tr.	1.112	0.746
7	1200	100	0	Cyl.	0.714	0.489
8	1200	120	0.5	Cyl.(Tp.)	0.569	0.264
9	1200	140	-0.5	Tr.	0.592	0.279

the tafel graphs for the corrosion current ( $I_{corr}$ ) and corrosion rate (Corr. rate) for each of the test specimens.

### 3.0 Result and Discussion

The Potentio-dynamic corrosion characterization calculates the corrosion current and rate for various friction stir weld specimens. Figures 3, 4, and 5 show the Tafel graphs for the corrosion current ( $I_{corr}$ ) and corrosion rate (Corr. rate) for each of the test specimens.

The corrosion characterization and subsequent derivation of corrosion current and corrosion rate is based on Tafel equation for electrochemical kinetics relating the over potential to current density.

$$\eta = A \times \log_{10} \left( \frac{i}{i_0} \right) \quad \dots (1)$$

Where,  $\eta$  is over potential,  
 $i_0$  is exchange current density,  $A/m^2$   
 $A$  is Tafel Slope  
 $V$ ,  $i$  is current density,  $A/m^2$ .

The corrosion values for FSW specimens are listed in Table 4, and the observations clearly show that the corrosion current and corrosion rate drop as the rotational speed is increased to 1200 rpm, the feed rate is increased to 140 mm/min, and the tool offset is reduced to -0.5 mm. Furthermore, the triangular pin profile is discovered to be the best pin profile for friction stir welding of the specimens with the least amount of corrosion current and rate. The fluctuation of corrosion current and corrosion rate for different process parameters is depicted in graphs in Figures 3, 4, 5, 6, and 7, respectively. Further, the surface morphology of the corroded surfaces are studied and the reason for the variation in corrosion current and

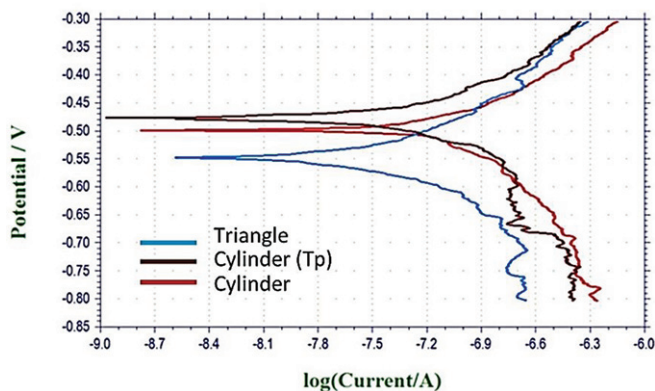


Figure 3: Graph representing Potential (V) versus log (Current) for rotational speed of 800 rpm

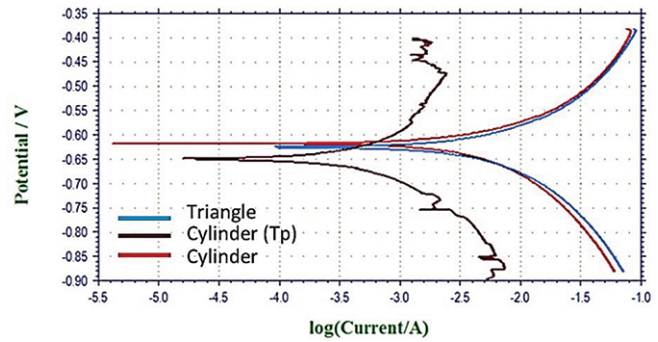


Figure 4: Graph representing Potential (V) versus log (Current) for rotational speed of 1000 rpm

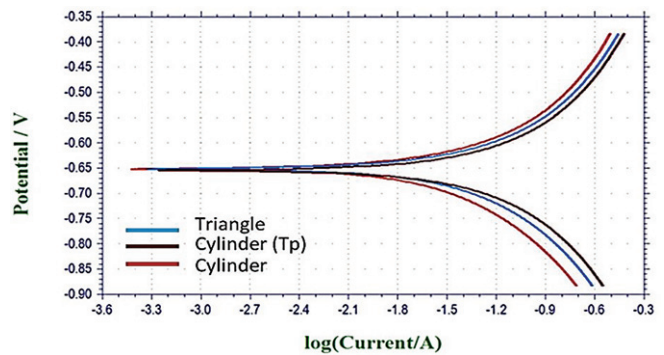


Figure 5: Graph representing Potential (V) versus log (Current) for rotational speed of 1200 rpm

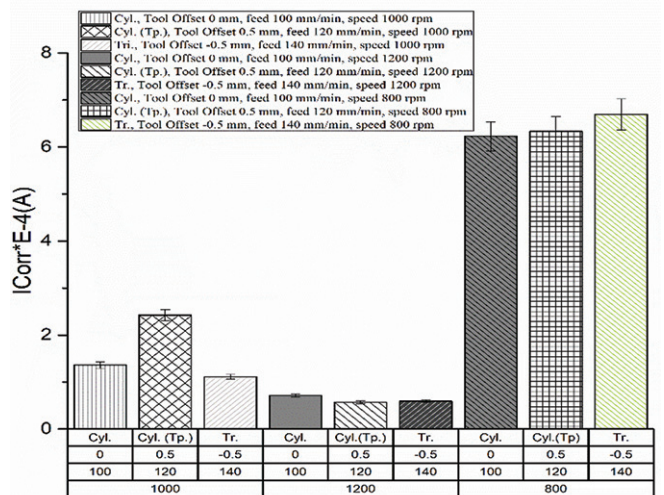


Figure 6: Bar chart with error bar showing the fluctuation of Corrosion current  $E-4$  (A)

corrosion rate are clearly understood through the microstructural images in Figure 8.

The surface morphology of the corroded surfaces for specimens of experimental trial 1, experimental trial 5 and experimental trial 9 are given in Figure 8(a),

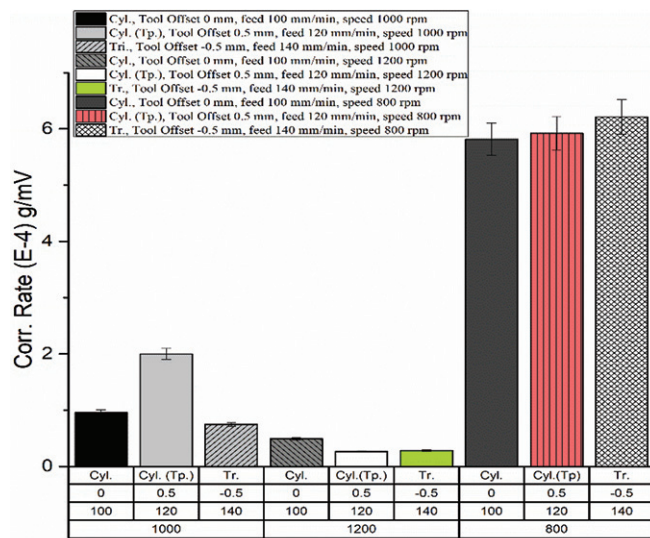


Figure 7: Graph showing the fluctuation of corrosion rate E-4 (g/mV)

reiterated the fact that the secondary processing operations brings about microcoring and segregation that inhibits the subgranular pitting reaction and thereby reduces the rate of corrosion [17]. Rami Alfattani et al., have further studied the corrosion behaviour of the friction stir weld specimens and have revealed that the microstructural refinement at the weld zone exhibits better corrosion resistance than the base metal, due to the zonal refinement and better bonding between the atoms leading to the reduction in the crevices and imperfections, thereby reducing the corrosion at the interface [18]. Koilraj M et al., have ascertained the influence of microstructural variations on the friction stir weld specimens, they have reported that the corrosion reduces in the friction stir weld zones due to the interatomic zonal interactions that leads to the higher rate of passive layer formations, which reduces the rate of corrosion in the FSW specimens [19].

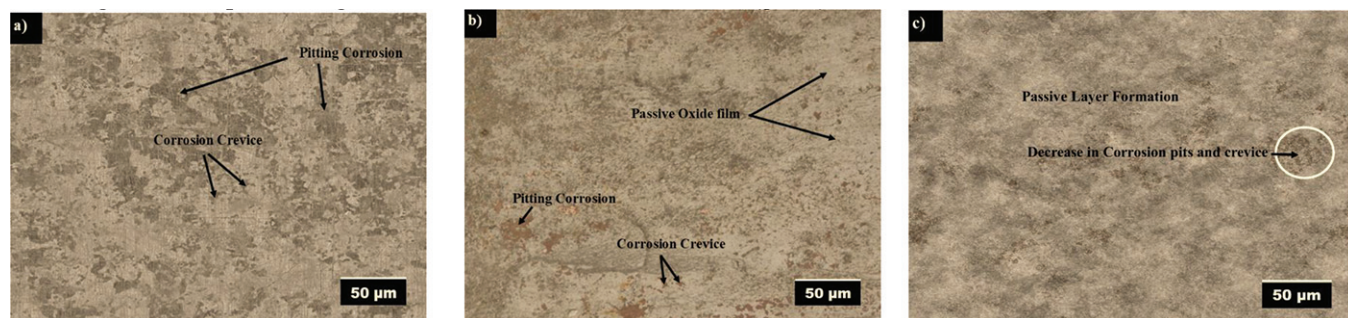


Figure 8: Microstructural images of the surface morphology of the corroded surfaces of (a) Specimen of experimental trial 1, (b) Specimen of experimental trial 5, (c) Specimen of experimental trial 9

8(b) and 8(c) respectively. The surface morphology of the corroded surface of the three different specimens captured at 200x, clearly reveals that there is corrosion pits and crevices which are predominant in the specimens friction stir weld at 800 rpm (Figure 8 (a)), and as the rotational speed of friction stir welding is increased to 1000 rpm and 1200 rpm, the corrosion rate decreases due to the formation of passive oxide film as in the specimen of experimental trial 5 (Figure 8 (b)) and subsequently a passive layer as in the specimen of experimental trial 9 (Figure 8 (c)).

The findings of the microstructural evaluation of the corroded surfaces are in line with the findings of Santhosh N et al., who have reported that the formation of the oxide films on the aluminium surface inhibits further corrosion due to the passivation of the surface layer towards the catalytic reactions [16]. Further, the works of Ramesha K et al., on the corrosion of the friction stir weld surfaces have

Thus, from the experimental findings and its validation with the literature on corrosion characterization of the friction stir weld specimens, it is herewith noted the process brings about transformation in the microstructural characteristics that influence the corrosion rate of the specimens due to strong bonding, microcoring and zonal passivation that reduces the corrosion due to the early formation of an oxide film that avoids further oxidation due to the resistance offered by the passive layer.

## 4.0 Conclusions

The corrosion resistance qualities of the specimens improve with increased rotational speed, feed, and for triangular tool pin profile and tool offset of -0.5 mm, according to the critical assessment of the corrosion characterization data. The corrosion current decreases

from 6.689 A to 0.569 A for rotational speed of 800 rpm, feed of 140 mm/min, triangular tool pin profile, while the corrosion rate decreases from 6.212 g/mV to 0.264 g/mV, this is majorly due to the formation of passive oxide layer at higher speed, feed and negative tool offset. The corrosion morphology depicted through the microstructure reveals that the passive layers are formed for friction stir weld specimens with the increase in feed, speed and use of triangle tool pin profile with -0.5 mm tool offset, which eventually inhibits the formation of corrosion crevices and corrosion pits.

## References

- [1] Hassan Abd El-Hafez, Abla El-Megharbel, "Friction Stir Welding of Dissimilar Aluminum Alloys", *World Journal of Engineering and Technology*, vol. 6, pp. 408- 419, 2018.
- [2] Jitender Kundu, Hari Singh, "Friction Stir Welding of Dissimilar AL alloys: Effect of process parameters on mechanical properties", *Engineering Solid Mechanics*, vol.4, pp.125-132, 2016.
- [3] Sadesh P, Venkatesh Kannan M, Rajkumar V, Avinash P, "Studies on Friction Stir welding of AA2024 and AA6061 dissimilar metals", *Procedia Engineering*, vol.75, pp.145-149, 2014.
- [4] K, Ramesha, Sudersanan PD, Santhosh N, and Sasidhar Jangam. 2021. "Design and Optimization of the Process Parameters for Friction Stir Welding of Dissimilar Aluminium Alloys". *Engineering and Applied Science Research* 48 (3):257-67. <https://ph01.tci-thaijo.org/index.php/easr/article/view/241021>
- [5] H.M. Rao," Effect of process parameters on mechanical properties of friction stir spot welded magnesium to aluminum alloy", *Materials and Design*, pp 235-245, 2015.
- [6] N.F.M Selamat, A.H Baghadi, Z. Sajuri, "Friction Stir welding of similar and dissimilar aluminum alloys for automotive application", *International Journal of Automotive and Mechanical Engineering*, vol.13, pp.3401-3412, 2016.
- [7] Santhosh N, Ramesha K, Mechanical and Thermal Characterization of Friction Stir Weld Joints of Al-Mg Alloy, *International Journal of Research in Aeronautical and Mechanical Engineering*, ETME Conference Issue, Cauvery Institute of Technology, Mandya, Dec 22-23, 2017.
- [8] Ramesha K., Sudersanan P.D., Santhosh N., Ravichandran G., Manjunath N. Optimization of Friction Stir Welding Parameters Using Taguchi Method for Aerospace Applications. *Advances in Structures, Systems and Materials. Lecture Notes on Multidisciplinary Industrial Engineering*. Springer, Singapore, pp 293 -306, 2020.
- [9] Santhosh N, U N Kempaiah, Ashwin C Gowda, Corrosion Characterization of Silicon Carbide and Fly Ash Particulates Dispersion Strengthened Aluminium 5083 Composites. *Journal of Catalyst & Catalysis*. 4(2): pp 9 – 21, 2017.
- [10] Sadashiva. M, H. K. Shivanand, Rajesh. M, Santhosh. N, Corrosion Behaviour of Friction Stir Welded Al 6061 Hybrid Metal Matrix Composite Plates, International Conference on Advances in Mechanical Engineering Sciences (ICAMES-17), PESCE, Mandya, Karnataka, India, 21 – 22 April 2017.
- [11] Ramesha, K., Santhosh, N., Kiran, K. et al. Effect of the Process Parameters on Machining of GFRP Composites for Different Conditions of Abrasive Water Suspension Jet Machining. *Arab J Sci Eng* 44, 7933–7943 (2019). <https://doi.org/10.1007/s13369-019-03973-w>
- [12] Santhosh N, Ranganadh Y, Satya Akash, Riti Mishra, U N Kempaiah, Ashwin C Gowda, Characterization of Aluminium 5083/SiCp/Fly Ash Hybrid Composites for Corrosion Behaviour in alkaline and acidic Medium for Potential Applications in Aerospace Components, Current trends in Carbon materials (IICS-BC & CTC), Rolls Royce Hall, AeSI, Bangalore, 08 April 2017.
- [13] Santhosh N, Manjunath N, Mahesh H R, Potentiodynamic Corrosion Characterization of Hybrid Aluminium Composites for Advanced Engineering Applications, *International Journal of Engineering and Advanced Technology (IJEAT)*, Vol9 Issue-3, pp.1434-1437, February, 2020. DOI: 10.35940/ijeat.C5025.029320.
- [14] K. Ramesha, P. D. Sudersanan, A. C. Gowda, N. Santhosh, S. Jangam and N. Manjunath. 2022. Friction Stir Welding of Dissimilar Aluminium Alloys for Vehicle Structures, *Int. J. Vehicle Structures & Systems*, 14(1), 5-9. doi:10.4273/ijvss.14.1.02.
- [15] Santhosh N, Kempaiah U N, Ashwin C Gowda, Srilatha Rao, Gurumoorthy Hebbar, Evaluation of Corrosion Mechanics of Silicon Carbide and

- Fly Ash Reinforced Hybrid Aluminium Metal Matrix Composites, International Conference on Emerging Research in Civil, Aeronautical & Mechanical Engineering, ERCAM 2017, pp 214 – 218, July 21 2017, Nitte Meenakshi Institute of Technology, Bengaluru, India.
- [16] Ramesha K, Sudersanan, P D, Santhosh N, Sasidhar Jangam. 2021. "Corrosion Characterization of Friction Stir Weld Joints of Dissimilar Aluminum Alloys.", EAI/Springer Innovations in Communication and Computing. <https://eudl.eu/doi/10.4108/eai.16-5-2020.2304097>
- [17] Alfattani, R.; Yunus, M.; Mohamed, A.F.; Alamro, T.; Hassan, M.K. Assessment of the Corrosion Behaviour of Friction-Stir-Welded Dissimilar Aluminum Alloys. *Materials* 15, 260, 2022. <https://doi.org/10.3390/ma15010260>.
- [18] K. Ramesha, P. D. Sudersanan1, Prem Kumar Mahto, Shaikh Mohammed Ismail, Ashwin C. Gowda, N. Santhosh, and V. Umesh. Influence of heat treatment on the tensile and hardness characteristics of friction stir weld joints of dissimilar aluminium alloys. AIP Conference Proceedings 2421, 030001 (2022)
-